Available online at www.sciencedirect.com
ScienceDirect
Tetrahedron 63 (2007) 9810–9824
Tetrahedron

The absolute axial configurations of knipholone and knipholone anthrone by TDDFT and DFT/MRCI CD calculations: a revision

Gerhard Bringmann,* Katja Maksimenka, Joan Mutanyatta-Comar, Michael Knauer and Torsten Bruhn

Institut für Organische Chemie, Universität Würzburg, Am Hubland, D-97074 Würzburg, Germany

Received 12 April 2007; revised 3 July 2007; accepted 3 July 2007
Available online 10 July 2007

Abstract—Triggered by a seemingly inconsistent twisting direction in the atroposelective ring cleavage reaction of biaryl lactones by using the 'lactone concept', the absolute axial configurations of the most important phenylanthraquinones, knipholone (**1**), and knipholone anthrone (**2**) were reassigned on the basis of renewed quantum chemical circular dichroism (CD) calculations using advanced, higher-level methods, viz. a time-dependent DFT (TDDFT) and a multireference configurational interaction approach (DFT/MRCI). Additional confirmation of the new configurational assignment of **1** and **2** was achieved by their stereochemically unambiguous interconversion, and further corroborated by the transformation of **1** into an 'leuco' phenylanthracene derivative **3**, i.e., a compound with a substantially different chromophore, whose absolute configuration was independently assigned again by quantum chemical CD calculations. Accordingly, the dextrorotatory enantiomer of knipholone, (+)-**1**, and its anthrone, (+)-**2**, has the *P*-configuration, while the laevorotatory forms, (−)-**1** and (−)-**2** (which likewise exist in nature), are *M*-configured. From this new configurational assignment, the absolute axial stereostructures of a whole series of further naturally occurring phenylanthraquinones may now be deduced.

1. Introduction

Knipholone (**1**)[1] and knipholone anthrone (**2**)[2] are the most prominent representatives of the phenylanthraquinones (Fig. 1). These naturally occurring biaryls, which have initially been discovered by Steglich, Dagne, and Yenesew in 1984 and 1993, are fascinating in many respects: structurally, because of their rotationally hindered and thus configurationally stable biaryl axis, which gives rise to atropo-enantiomers (or, in the case of glycosides, atropo-diastereomers), biosynthetically, because their two molecular portions, the anthraquinone part and the trioxyacetophenone moiety, are built up from eight and four acetate units, respectively,[3] and pharmacologically, because they display significant antimalarial[4] and antitumor[5] activities as well as antioxidant[6] properties, along with an inhibition of leukotriene formation.[7] Remarkably, the antitumoral activities of natural phenylanthraquinones significantly depend on

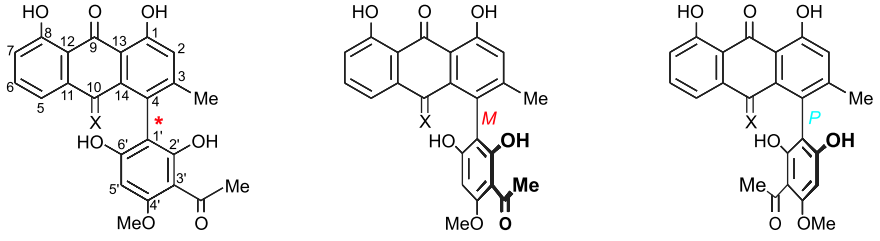

1 X = O
2 X = H_2
(*M*)-**1** X = O
(*M*)-**2** X = H_2
(*P*)-**1** X = O
(*P*)-**2** X = H_2

Figure 1. Constitutions of knipholone (**1**) and knipholone anthrone (**2**), and their possible atropo-enantiomeric forms, (*M*)- and (*P*)-**1** and (*M*)- and (*P*)-**2**.

Keywords: Knipholone; Knipholone anthrone; Quantum chemical CD calculations; Axial chirality; Absolute configuration.
* Corresponding author. Tel.: +49 931 888 5323; fax: +49 931 888 4755; e-mail: bringman@chemie.uni-wuerzburg.de

0040–4020/$ - see front matter © 2007 Elsevier Ltd. All rights reserved.
doi:10.1016/j.tet.2007.07.001

the absolute configuration at the biaryl axis,[5] showing the importance of axial chirality in these and other[8] biaryls. This stereochemical aspect seems to be substantial for the phenylanthraquinone-producing plants, too: as an example, knipholone (**1**) and its 6′-*O*-sulfate, although co-occurring in the same plant, have the opposite axial configurations.[9]

Given the importance of axial chirality for these compounds, we investigated the absolute axial configuration of **1** and **2** by quantum chemical CD calculations at a semiempirical level in 1999 and deduced the main (dextrorotatory) atropo-enantiomers of both, **1** and **2**, to be *M*-configured.[10]

In view of this stereochemical assignment, the result of our first, atropo-enantioselective total synthesis of both **1** and **2**,[11,12] following our 'lactone concept',[13,14] was unexpected. The ring cleavage reaction of the respective configurationally unstable biaryl lactone intermediate, when using the *R*-enantiomer of the CBS reagent, which would have been expected to lead to the assumed axial *M*-configuration of (+)-knipholone, actually gave the 'wrong', laevorotatory enantiomer of the natural product. This seemed to hint at a non-predictability of the ring cleavage direction within the 'lactone method'. Still, this has, ever since, remained the only exception to the—otherwise fully consistent—stereochemical course of all such lactone cleavage reactions. A second inconsistency originated from the renewed isolation of **1** and **2** with varying enantiomeric ratios (according to LC–CD) from diverse sources and, in particular, with a higher chemical purity; these samples provided CD spectra different from those initially measured, i.e., from the curves that had been the basis for the configurational assignment in 1999. The pretendedly inconsistent lactone cleavage direction and the new CD measurements, together with the more accurate computational methods available meanwhile, warranted a systematic re-investigation of the absolute configurations of knipholone (**1**) and knipholone anthrone (**2**).

In this paper, we report on the renewed investigation of the absolute configuration of **1** and **2** by using advanced quantum chemical CD calculations based on time-dependent DFT (TDDFT) and multireference configurational interaction (DFT/MRCI) approaches, reassigning the naturally predominant, dextrorotatory enantiomers of knipholone, (+)-**1**, and knipholone anthrone, (+)-**2**, as both being *P*-configured. This stereochemical attribution was further corroborated by converting **1** into the related likewise axially chiral phenylanthracene derivative **3** (Fig. 2), i.e., a compound with a substantially different chromophore, and its independent configurational assignment, again as *P*.

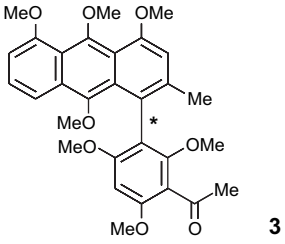

Figure 2. Structure of the semisynthetic phenylanthracene derivative **3** of knipholone (**1**).

2. Results and discussion

2.1. The stereochemical course of the ring cleavage of configurationally unstable biaryl lactones within the 'lactone concept'

A first hint at a possibly wrong configurational assignment of **1** and **2** by the early quantum chemical CD calculations resulted from the above-mentioned unexpected stereochemical course of the first (and as yet only) total synthesis of **1** and **2**. The key step of this synthesis was the atropo-enantioselective ring cleavage reaction of the configurationally unstable biaryl lactone precursor **4** by using the CBS system (Scheme 1a). From previous experience with quite a broad spectrum of different related model biaryl lactones **A**[14] (Scheme 1b) and from the application of this methodology to a series of most diverse natural biaryls, among them mastigophorenes A and B,[15] the vancomycin biphenyl fragment,[16] and a variety of mono- and dimeric naphthylisoquinoline alkaloids (i.e., dioncopeltine A,[17] korupensamines A and B,[18] and others[13,19,20]), the expectation was that virtually any lactone **A**, when opened with the CBS system (oxazaborolidine **5**·BH_3) would lead to a product **B**, i.e., with the phenolic OH group down, when using (*S*)-**5** (Scheme 1b, top), and to *ent*-**B**, with the OH group up, when using (*R*)-**5** (Scheme 1b, bottom). For the synthesis

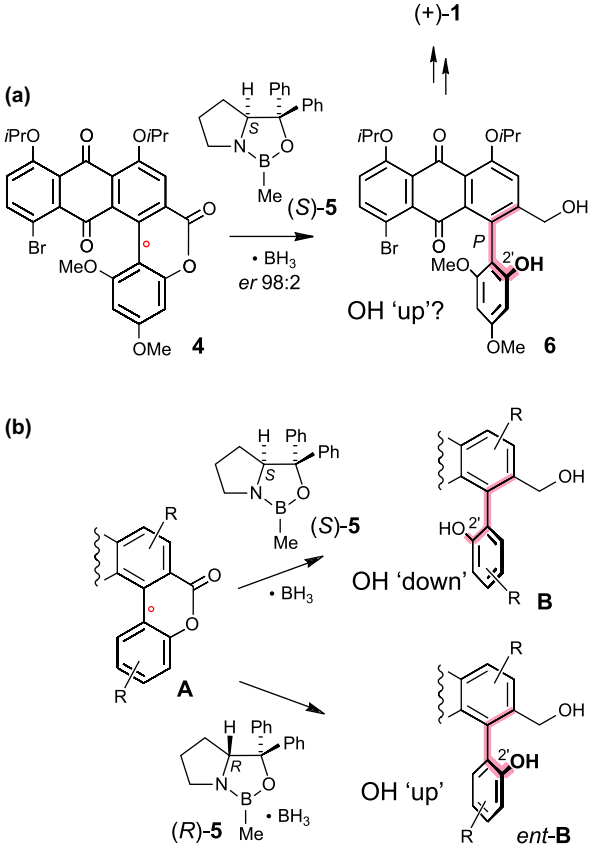

Scheme 1. The questionable (yet initially assumed) stereochemical course of the atroposelective lactone-ring opening of the 'knipholone lactone' **4** with the (*S*)-CBS reagent **5** as the key step in the first total synthesis of knipholone (**1**), supposedly leading to the *P*-configured product **6**, i.e., with the OH group 'up', as expected from the previously assigned *M*-configuration of (+)-knipholone (**1**) (a), and 'usual' (as yet reliably consistent) stereochemical course with other biaryl lactones (b), as a result of a broad series of examples from different groups.[13,14,19,21,22]

of (+)-**1**, with its assumed *M*-configuration, i.e., with 2′-OH up (Scheme 1a), however, the consequently used *R*-enantiomer of **5** actually led to the opposite (laevorotatory) enantiomer of **1**, so that the other oxazaborolidine enantiomer, (*S*)-**5**, had to be used to reach the natural product (+)-**1**. This unexpected ring cleavage direction was—unfortunately—not recognized as a hint at a wrong configurational assignment of **1**, but was just interpreted as an exception to the above-mentioned rule. However, since all previous (see above) and later[20–23] examples of atroposelective ring cleavage reactions with biaryl lactones of most different structures, under most different conditions,[14,19,20,24,25] including the work by others who applied the lactone method for the total synthesis of, e.g., steganones,[21,23] the question arose whether really the ring cleavage of **4** was the only—and thus not understandable—exception, also in view of quantum chemical investigations on the stereochemical course of such reactions,[26] or whether possibly indeed the lactone-ring opening reactions were consistent, but the configurational assignment of **1** and **2** was wrong.

2.2. Renewed experimental circular dichroism investigation of knipholone (1) and knipholone anthrone (2)

A second hint at the necessity to re-investigate the initial configurational assignment of **1** and **2** was the much better quality of the CD spectra obtained more recently from renewed isolation work from a broad variety of different plants (even including cleavage products of novel-type dimeric representatives[27]).

Improved isolation techniques did indeed allow us to generate highly pure samples and thus reproducible CD spectra for all new isolates. The newly measured spectra were now virtually identical, but in part different from the previously reported ones. Thus, while the new CD spectrum of knipholone (**1**) showed only minor differences (broad, low-intensity bands at about 350 and 430 nm possessing a positive sign), more substantial changes were observed in the case of the chemically less stable knipholone anthrone (**2**), viz. two additional intense CD signals above 280 nm, which could not be seen in the old spectrum of **2**. Further CD measurements of **2** in different solvent systems (Fig. 3d) proved the authenticity of this spectrum. These spectral differences may certainly be ascribed to a partial decomposition already after a short time, which can be reproduced, e.g., just by keeping a sample of **2** (Fig. 3e) for 2 h at daylight in methanol at room temperature, leading to considerably changed curves, yet resembling those that had been used for the comparison with the theoretically predicted CD spectra in 1999.

The re-measured spectrum of **2** gave rise to further doubts about the correctness of the previous configurational attribution, since the CD couplet with the first positive Cotton effect (CE) at 300 nm and the second negative one at 280 nm of almost identical intensities resembled a classical exciton couplet arising from the interaction between the acetophenone[28] and anthrone[29,30] chromophores. According to the exciton chirality method,[31] this CD split should indicate a ‘positive chirality’, here corresponding to a *P*-configuration of **2**, whereas the structure of *M*-configured knipholone anthrone

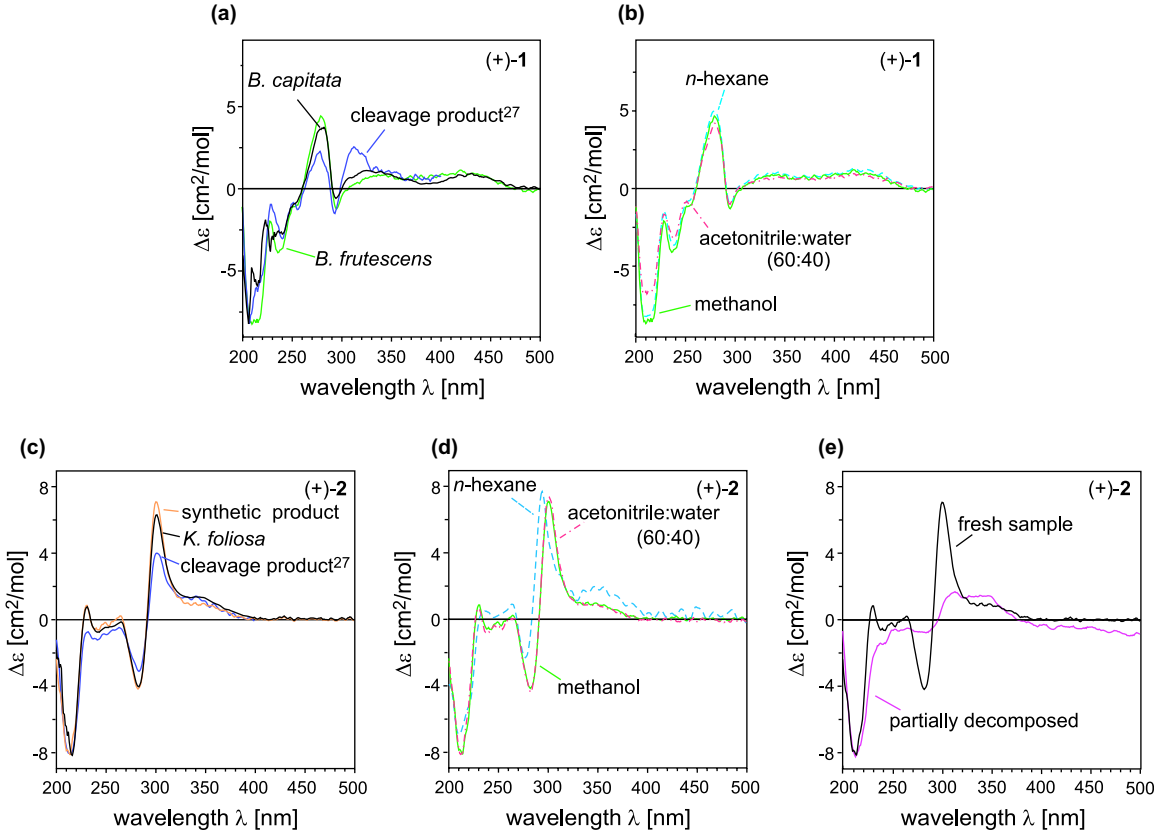

Figure 3. Experimental CD spectra of (+)-knipholone [(+)-**1**] (a) and (+)-knipholone anthrone [(+)-**2**] (c) of different origins (in methanol) and those measured in various solvent systems (b, d); comparison of the CD spectra of freshly dissolved knipholone anthrone (**2**) and the partially decomposed sample of **2** (e).

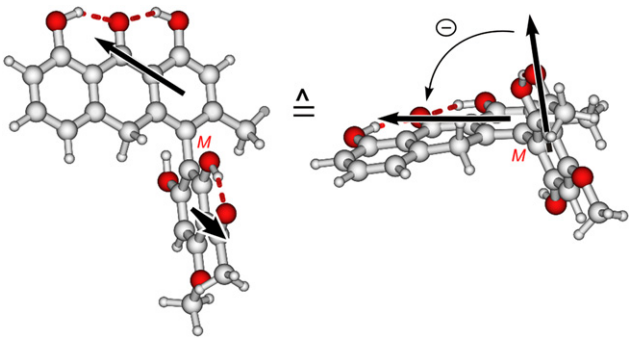

Figure 4. Expected negative Cotton effect for (*M*)-knipholone anthrone (**2**) with its 'negative chirality', following the exciton chirality method. The arrows schematically indicate the directions of the electric transition dipole moments in the acetophenone and anthrone chromophores.

(as hitherto assumed for the dextrorotatory form of **2**) would be expected to be a case of a 'negative chirality' (Fig. 4).

Therefore, to finally clarify the configurational assignment at the biaryl axes of both knipholone anthrone (**2**) and knipholone (**1**), comprehensive, more in-depth theoretical and experimental investigations had to be carried out.

2.3. TDDFT and DFT/MRCI circular dichroism calculations for knipholone (1)

For the renewed investigations of the absolute configurations of **1** and **2**, their CD spectra were again calculated, but now using more advanced methods, viz. a time-dependent DFT (TDDFT) approach[32–35] and a multireference configuration interaction procedure (DFT/MRCI).[36] In analogy to our previous theoretical work,[10] the present calculations were performed for the *M*-enantiomers of **1** and **2**, starting with the molecule of the phenylanthraquinone, knipholone (**1**). The conformational analysis of **1**, which was likewise carried out at the semiempirical PM3 level,[37] resulted in the same 12 conformers as reported previously.[10] Further optimization of these structures by the DFT-based RI-BLYP/SVP method[38–41] revealed only one additional relevant low-energy conformer within an energy cut-off of 3 kcal/mol above the presumable global minimum. The two minima thus found just differed in the dihedral angle θ_{ABCD} at the biaryl axis, with a value of $-109°$ in the global minimum conformer and $-79°$ in the second minimum structure. The global minimum is stabilized by the formation of a strong hydrogen bond (d_{O-H} 1.70 Å) between the hydroxy function at C-6′ and the carbonyl at C-10 (Fig. 5, left).

In these DFT-based calculations, the obtained conformers did not show the pronounced 'concave'/'convex' curvatures of the anthraquinone ring of **1**, as had been found in the previous (semiempirical) calculations,[10] but rather exhibited an almost planar orientation, yet with a small degree of distortion due to the presence of the hydrogen bond in the global minimum structure, while in the second conformer of **1** the anthraquinone ring was fully planar. Again different from the semiempirical results, the acetyl group at C-3′ revealed only one energetically preferred orientation, viz. lying in the phenyl plane, with formation of a hydrogen bond to the hydroxy function at C-2′. These conformational arrays

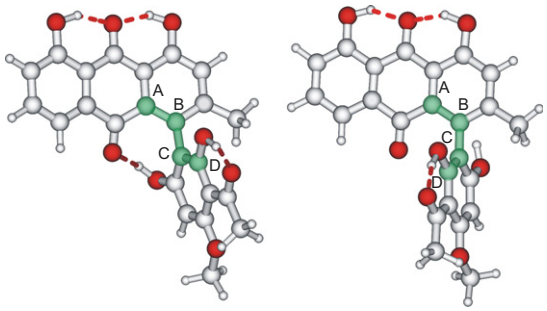

conf1 (θ_{ABCD} -109°) *conf2* (θ_{ABCD} -79°)

$\Delta\Delta H_f$[kcal/mol]	*conf1*	*conf2*
BLYP/SVP	0.00	1.31
BLYP/TZVP	0.00	0.39
B3LYP/TZVP	0.00	0.16
g_i^{B3LYP}	0.57	0.43

Figure 5. Two minimum structures of the *M*-enantiomer of knipholone, (*M*)-**1**, differing in the dihedral angle at the biaryl axis, the relative energies of these two conformers as calculated by the BLYP/SVP, BLYP/TZVP, and B3LYP/TZVP methods, and the weighting factors for the B3LYP optimized structures.

constitute an important issue, since the geometries of the chromophoric frameworks, i.e., the anthraquinone portion and the acetophenone ring, and their orientations appear critical for the quality of the subsequently calculated excited-state wavefunctions, and hence for the resulting accuracy of the final CD spectrum. Therefore, the two minima of **1** were further optimized by applying a better method[42] without the RI approximation and by using a significantly enlarged basis set, namely B3LYP/TZVP[40,43,44] (for the respective energy differences, see Fig. 5). The observed large difference between the BLYP/SVP- and B3LYP/TZVP-based relative energies of the two conformers of **1** is related to the basis set used, predominantly, rather than to the functional. Thus, the optimizations at the BLYP/TZVP level reduced the relative energy difference to 0.39 kcal/mol, which is nearer to the B3LYP-based results. The same tendency was observed for compound **3** (see below).

The excited-state energy calculations were performed with a time-dependent DFT method by using the same B3LYP functional and TZVP basis set, and by a DFT/MRCI approach[36] with the standard BHLYP hybrid functional[45] and the SVP atomic orbitals basis (configuration-selection cut-off=$0.8E_h$[46]). In the case of the DFT/MRCI calculations, the use of a larger basis set, e.g., TZVP,[44] was not possible because of the high computational costs. Since the TDDFT calculations resulted in a very similar CD pattern for each conformer of **1** (Fig. S1, Supplementary data), the more demanding DFT/MRCI calculations were carried out only for the global minimum structure. The single TDDFT and MRCI based CD and UV curves were obtained by using a Gaussian shape function (for details, see Section 4), and the resulting spectra of the individual conformers were then added up in a Boltzmann weighted manner. The resulting computed CD and UV spectra were then compared with the experimental curves of (+)-knipholone [(+)-**1**] (Fig. 6).

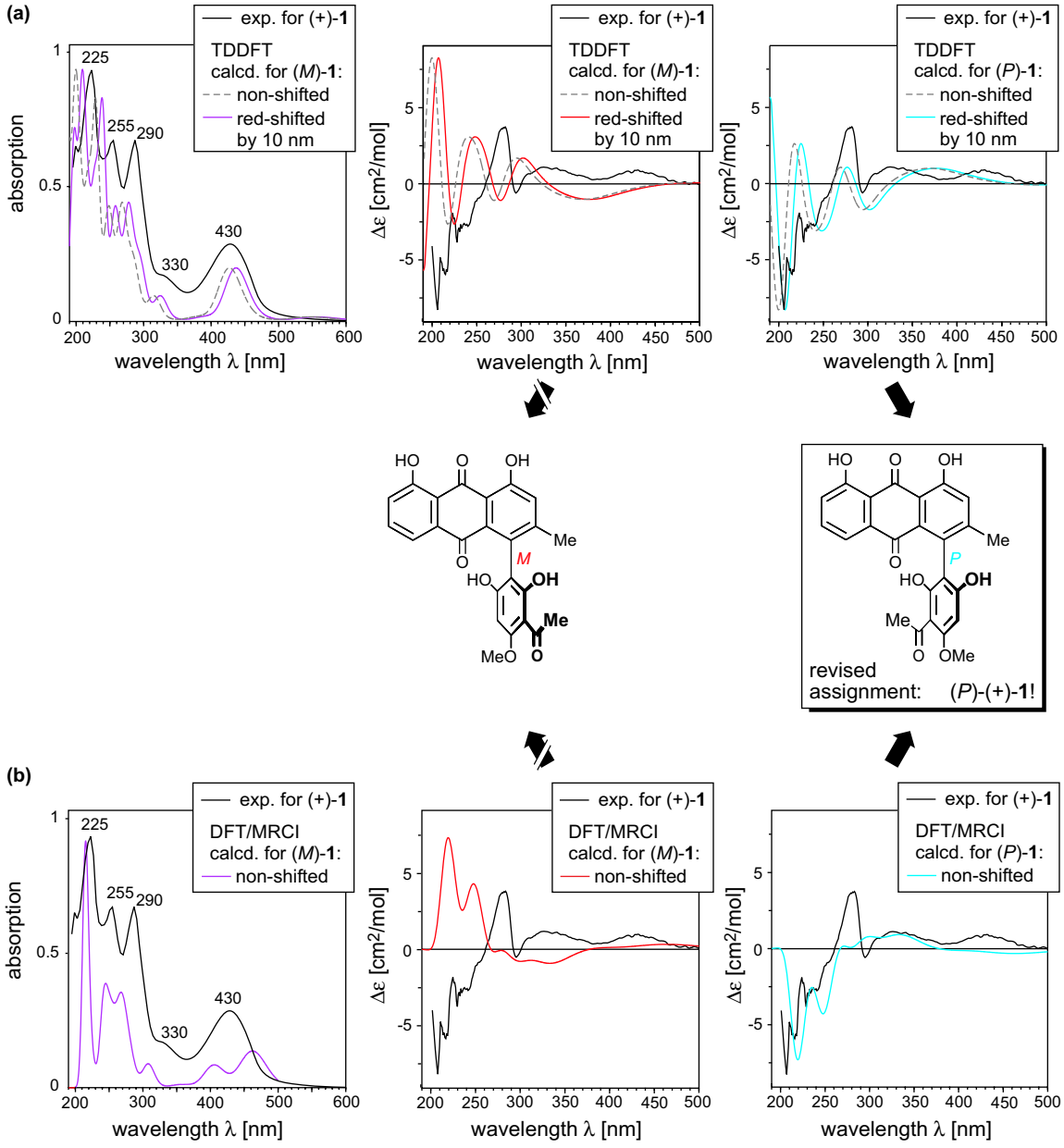

Figure 6. Results of the TDDFT (a) and DFT/MRCI (b) CD calculations for (*M*)- and (*P*)-**1**, and their comparison with the experimental CD spectrum of (+)-**1**; revised absolute axial configuration of (+)-knipholone (**1**) (center right).

Comparison of the measured UV curve of **1** with the TDDFT-based spectrum revealed that the calculated excitation energies were overestimated by approximately 0.2–0.3 eV (corresponding to 10 nm) with respect to the first three experimental UV bands located at 430, 330, and 290 nm, whereas an analysis of a spectral range from about 250 nm and below was difficult, since the TDDFT method may not predict this region with a sufficient accuracy due to a highly multiconfigurational character of the high-energy excitations.[46] For 'UV correction',[47] the corresponding CD spectra predicted for the two enantiomers of **1** were thus red-shifted by 10 nm, and were then compared with the measured CD spectrum of (+)-**1**. For reasons of clarity, Figure 6a shows the comparison with both the UV-corrected (solid lines) and the non-corrected (dashed lines) theoretical UV and CD spectra. The CD spectrum calculated for (*M*)-**1** showed an unambiguously opposite behavior in comparison to the experimental CD curve, whereas the spectrum predicted for the *P*-enantiomer matched the experimental one of (+)-**1** very well, including broad low-intensity bands at around 350 and 430 nm (Fig. 6a), thus clearly indicating that (+)-**1** is *P*-configured, and not *M* as initially assigned.[10,12]

The same results were obtained from the DFT/MRCI calculations. In this case, however, the UV correction seemed to be unnecessary or even unjustified, since the first experimental UV band at 430 nm, which corresponds to the HOMO–LUMO and (HOMO-3)–LUMO transitions, was predicted fairly correct, whereas the excitations belonging to the next three bands were overestimated in energy by 0.2 eV. Therefore, the theoretical UV and CD spectra of **1** were compared with the experimental data without any shift (Fig. 6b).

Despite the underestimated intensity of the second positive CD band at 270 nm, the CD spectrum of (*P*)-**1** reproduced the experimental spectrum with a reasonable accuracy, permitting to confirm the above revised absolute axial configuration of (+)-knipholone, (+)-**1**, as *P*.

The most probable reason for the former incorrect configurational assignment is the treatment of the molecule only at a semiempirical level or, in the case of the MD simulations, by simply using empirical force field calculations. This assumption was indirectly confirmed by the fact that even optimization of the ground-state structures at the RI-BLYP/SVP level for the ensuing CD calculations provided ambiguous results (Fig. S2, Supplementary data).

2.4. TDDFT and DFT/MRCI circular dichroism calculations for knipholone anthrone (2)

After having evidenced the apparently wrong initial attribution of the absolute configuration of knipholone (**1**) and with its now successful and unequivocal revision, the renewed quantum chemical calculation of the CD spectrum of knipholone anthrone (**2**), also in view of its now available new experimental spectra, had become a necessary and rewarding task. In analogy to knipholone, the conformational analysis of **2** was performed starting with the semiempirical PM3 method, with subsequent further optimization of the geometries obtained, at the RI-BLYP/SVP and B3LYP/TZVP levels. In the latter case, only one conformer of **2** was found (Fig. 7).

The CD and UV spectra of **2** were calculated by using the same approaches as described above for **1**. Comparison of the experimental UV curve of **2** with the theoretically predicted one showed that the first UV band observed at 350 nm was reproduced highly accurately by both methods, TDDFT and DFT/MRCI, whereas the excitations corresponding to the experimental bands at 290, 260, 230, and 215 nm were overestimated in energy by 0.3–0.4 eV (i.e., by 15 nm) (Fig. 8, dashed lines). The calculated UV spectra thus had to be shifted by 15 nm to higher wavelengths to match the first three experimental UV bands as much as possible (Fig. 8, solid lines). The same wavelength shift was applied to the theoretical CD spectra of **2**, which were then compared with the experimental CD curve of (+)-**2**.

But anyhow, irrespective of an application of the UV shift, the first two CD bands predicted for the *M*-enantiomer of knipholone anthrone (**2**) showed negative Cotton effects,

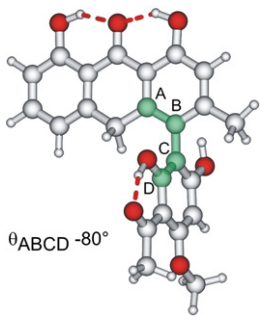

Figure 7. The global minimum structure of knipholone anthrone (**2**) as found by the B3LYP/TZVP method.

whereas in the experimental spectrum they had a positive sign (see also Section 2.1 and Fig. 3), indicating the opposite absolute configuration of (+)-**2**, i.e., *P*. Thus, while the TDDFT calculations were not able to entirely simulate the positive exciton couplet at around 300 nm (Fig. 8a), the DFT/MRCI/SVP based CD spectrum of (*P*)-**2** fully reproduced all features of the experimental CD curve of (+)-**2**, including the CD split (Fig. 8b). The new experimental spectra of pure (+)-**2** and the high-level calculations clearly indicate that the absolute configuration of (+)-**2** must be revised to be *P*, and not *M*, as assumed earlier.[10,12] This result is in agreement with the above-mentioned (see Section 2.1 and Fig. 4) positive CD couplet, which, following the exciton chirality method,[31] is indicative of the *P*-configuration of (+)-**2**.

2.5. Stereochemical identity of (+)-(*P*)-knipholone (1) and (+)-(*P*)-knipholone anthrone (2) by their semisynthetic interconversion

Additional support for the configurational assignment of **1** and **2** was expected from a chemical investigation of their stereochemically unambiguous interconversion, i.e., by reduction of (*P*)-**1** to give—if correctly assigned—(*P*)-**2**, and, vice versa, the oxidation of (*P*)-**2** to deliver (*P*)-**1**, to be analyzed by chromatography on a chiral phase with online CD coupling (LC–CD). Such a stereochemical identity of the axial configurations of **1** and **2** would be in line with the homochiral behavior predicted by the quantum chemical CD calculations, according to which both compounds in their dextrorotatory form should have the same absolute *P*-configuration. These investigations were complicated by the observed partial racemization of the compounds under the applied redox conditions, possibly due to the occurrence of phenoxy radical intermediates with lowered atropo-isomerization barriers. Thus, an enantiomerically pure (Fig. 9a) sample of synthetic (+)-knipholone anthrone [i.e., (*P*)-**2** according to the new, revised configurational assignment] was oxidized to knipholone (**1**, Fig. 9b) showing a ratio of 69:31 *P* to *M*, as compared to an authentic knipholone sample (Fig. 9c, 75:25 *P* to *M*) isolated from *Bulbine capitata*.[48] The latter 75:25 sample of (+)-knipholone (**1**) was in turn reduced to knipholone anthrone (**2**, Fig. 9d), whose major, more slowly eluting peak coeluted chromatographically (t_R=30 min) with the peak of enantiomerically pure anthrone, (+)-(*P*)-**2**, thus indicating its *P*-configuration (Fig. 9a and d). The interconversion shows that the more rapidly eluting peak of **2** (i.e., the minor reduction product) is *M*-configured, while in the case of knipholone (**1**) the *M*-enantiomer is the slower one. Due to the nearly racemic character of the knipholone anthrone obtained by reduction of (*P*)-(+)-knipholone (Fig. 9d), additional evidence for the identity of the respective peaks, and thus of the reversed HPLC behavior of **2** in comparison to **1**, was acquired by a spiking experiment by adding enantiopure knipholone anthrone to that near-racemic sample of **2** with subsequent chromatographical analysis by using HPLC–UV and HPLC–CD (for the respective diagrams, see Fig. S3 in Supplementary data). An analogous reversed chromatographic behavior of knipholone anthrone (**2**) in comparison to knipholone (**1**) itself is also been observed for isoknipholone and its anthrone (i.e., the respective 4′-hydroxy-6′-methoxy isomers of **1** and **2**[27] thus further demonstrating the value of the online LC–CD and LC–UV methodologies for the stereoanalysis of these

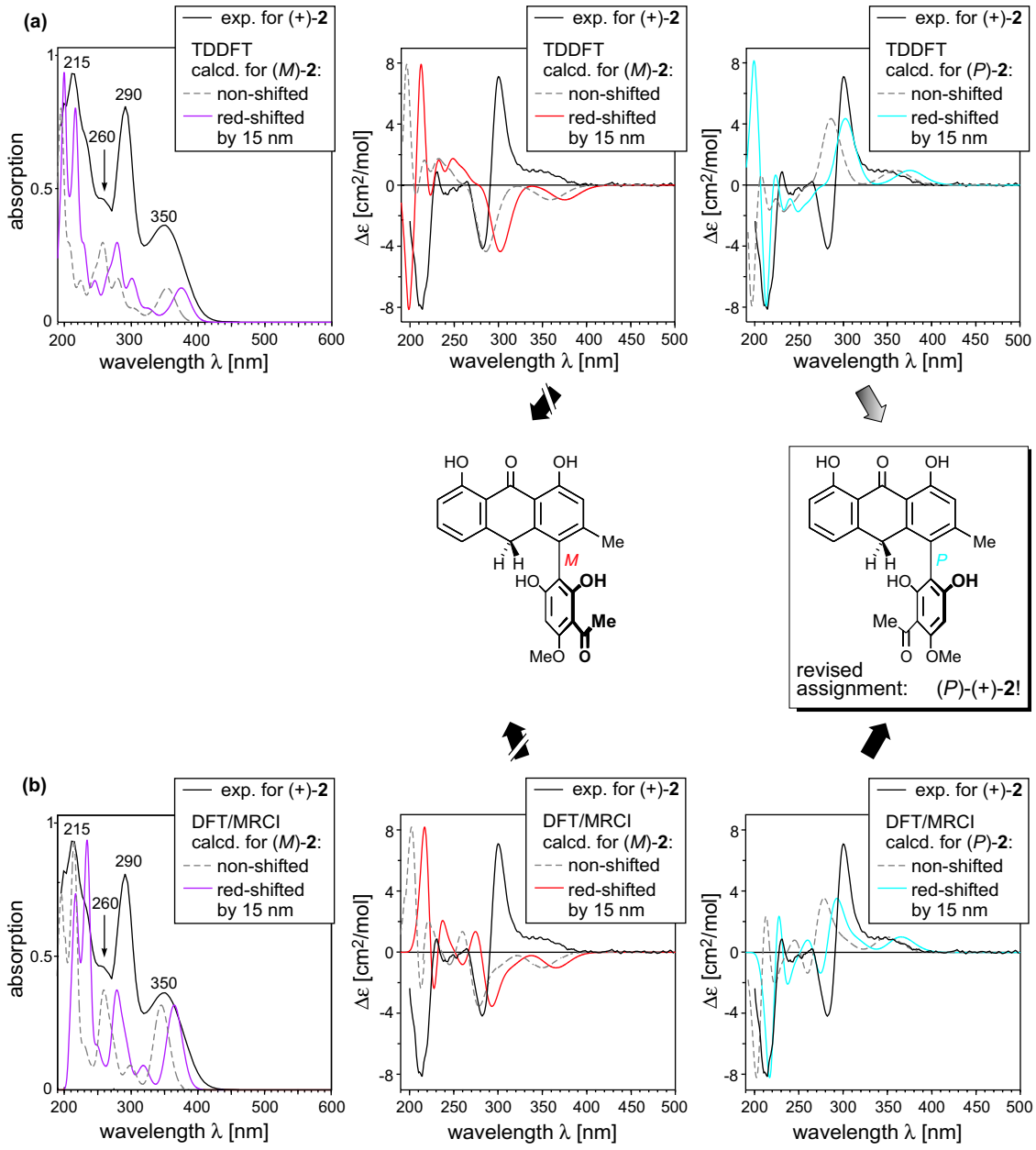

Figure 8. Revised assignment of the absolute axial configuration of (+)-knipholone anthrone (**2**) by TDDFT (a) and DFT/MRCI (b) calculations performed on the *M*-enantiomer of **2**.

compounds). The experiments prove the homochiral character of **1** and **2**, which is in line with the identical configuration of (+)-knipholone anthrone (**2**) and (+)-knipholone (**1**) now assigned independently to be *P* in both cases.

2.6. Further confirmation of the revised axial configuration of 1 (and thus 2) by independent CD investigations on its 'leuco' derivative 3

The above-described revised configurational assignment of (+)-knipholone, (+)-**1**, and (+)-knipholone anthrone, (+)-**2**, by high-level quantum chemical CD calculations in combination with experimental CD spectra taken on pure samples of **1** and **2**, warranted additional approaches to further prove this result. However, all attempts to crystallize appropriate derivatives of knipholone (**1**) equipped with chiral auxiliaries [like, e.g., the 6′-*O*-(1*S*)-camphor-10-sulfonate analog of **1**] or with 'heavy' atoms [like, e.g., the 6'-*O*-(1-bromo-2-naphthoyl) derivative of **1**] failed to give crystals of suited quality for an X-ray structural analysis, while both knipholone (**1**) and its likewise natural 4′-*O*-demethyl analog did provide crystals suited for an X-ray structural analysis, yet only in their racemic forms, selectively crystallizing out of the natural scalemic mixture.

In view of this unfavorable crystallization behavior of **1** and **2** and their derivatives, an independent configurational attribution was approached by the stereochemically unambiguous transformation of the phenylanthraquinone **1** into the respective phenylanthracene **3**, i.e., a derivative with a substantially different chromophore, whose absolute axial configuration was likewise established by quantum chemical

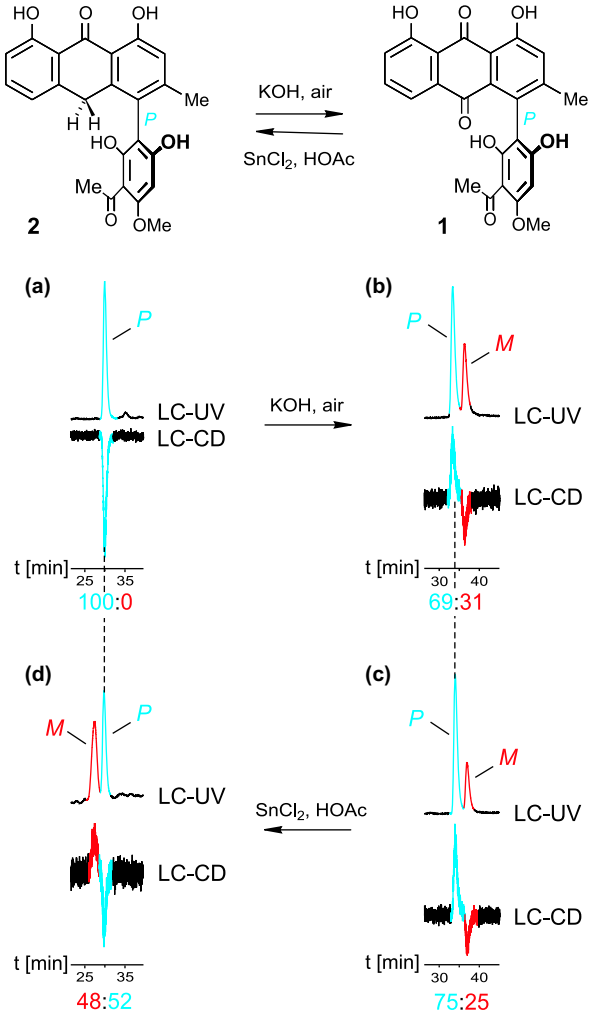

Figure 9. Proof of the stereochemical identity of (+)-knipholone (**1**) (b) obtained by oxidation of enantiomerically pure knipholone anthrone (100:0 *P* to *M*) (a), and, vice versa, enantiomeric resolution of knipholone anthrone (**2**) (d), obtained by reduction of authentic knipholone (75:25 *P* to *M*) (c).

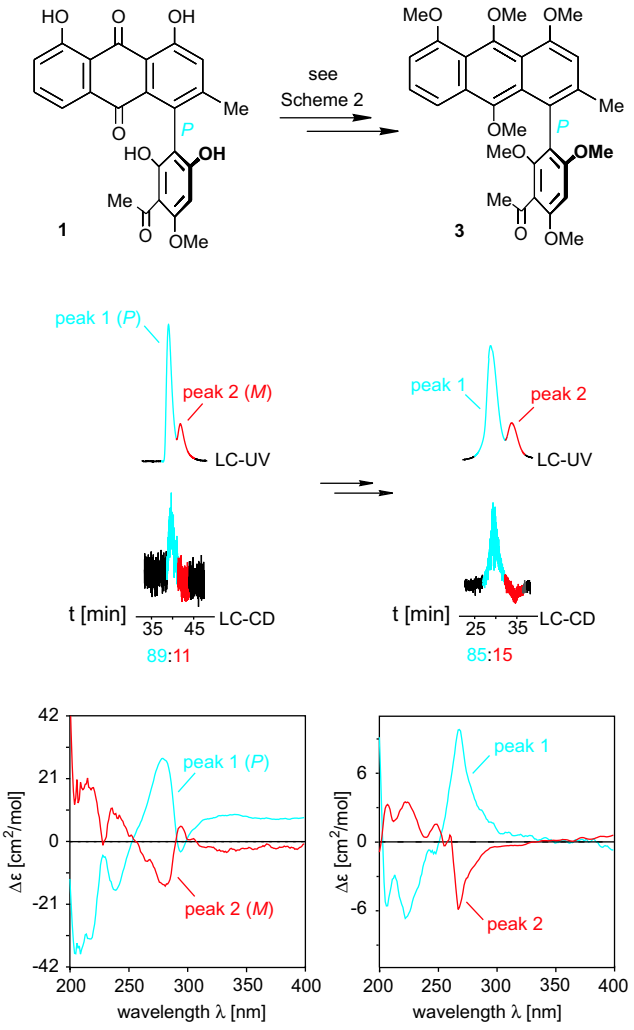

Figure 10. Determination of the enantiomeric ratio of the starting material (**1**, 89:11 *P* to *M*) and of the obtained product (**3**, 85:15 *P* to *M*) by HPLC–CD coupling on a Chiralcel OD-H column.

CD calculations. Among the different imaginable 'leuco' forms of **1** or **2**, i.e., with or without an oxygen function at C-10, compound **3** seemed most favorable from its simplified (and thus easier to interpret) anthracene chromophore as compared to that of **1** and **2**, from the additional conformational rigidity of the generated fully aromatic system, from an even more restricted torsion by the higher steric hindrance due to the methoxy group at C-10 as compared to a C-10-deoxy analog (when starting from **2**), and from its seemingly straightforward preparation. The synthesis of **3** is shown in Scheme 2.

For this, first preparation of such an as yet unknown axially chiral phenylanthracene **3**, the best-possible starting material of **1**, i.e., with the highest-available quantity and enantiomeric purity, was chosen, as available by isolation from *Bulbine frutescens*,[49] viz. (+)-knipholone (**1**) with an enantiomeric ratio of (+)- to (−)-**1** of 89:11. Furthermore, mildest-possible reaction conditions had to be chosen, to avoid further racemization of the material or even reductive cleavage of the axis.

Thus, although many different methods and conditions for the reduction of the hydroxy substituted anthraquinones

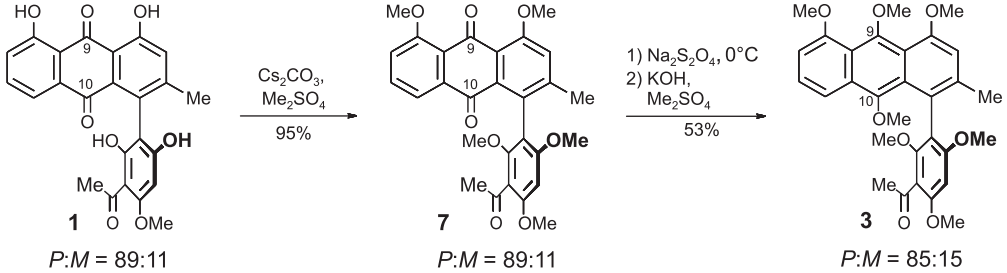

Scheme 2. Synthetic route to the 'leuco' derivative **3** of knipholone (**1**).

are described in the literature,[50–55] all of the free OH groups of knipholone (**1**) were first O-methylated under standard conditions[56] to give the pentamethyl ether **7**, by using Cs_2CO_3 and Me_2SO_4 in acetone (Scheme 2) to stabilize the molecule before reduction, thus avoiding the above-mentioned undesired side reactions.

In analogy to a protocol by Kraus and Man,[54] originally described for the reduction of free, phenyl-devoid anthraquinones, compound **1** was treated with sodium dithionite at 0 °C, with subsequent in situ O-methylation of the newly generated hydroxy groups at C-9 and C-10 to avoid a re-oxidation back to **7** during workup. To test whether the intermediate **7** and the final product **3** had remained stereochemically intact or whether partial or total racemization had taken place, online HPLC–UV monitoring of the product peaks was carried out after workup of each reaction step (Fig. 10). Accordingly, the O-methylation of **1** to **7** had not affected the initial 89:11 enantiomeric ratio, whereas the reduction decreased the ratio to 85:15 (*P* to *M*).

In the online measured CD spectra, the two peaks corresponding to the enantiomers of the obtained 'leuco' derivative **3** of knipholone (**1**) indeed showed a significantly simpler chiroptical behavior as compared to that of **1**, viz. a classical bisignated positive couplet for the first eluting peak hinting at the *P*-configuration, and a negative couplet in the case of the second eluting peak in agreement with the *M*-configuration of this slower enantiomer of **3**.

This tentative assignment was again confirmed by CD calculations. As in the above cases, the calculations were carried out for the *M*-enantiomer of **3**. The conformational analysis of (*M*)-**3** revealed three low-energy conformers lying within an energetic cut-off of 3 kcal/mol (Fig. 11). The obtained minima structures differed mainly in the orientation of the acetyl function at C-3′, which was now—since devoid of any hydrogen bonding—twisted out of the phenyl plane in either direction due to the steric hindrance by the methoxy substituent at C-2′ (Fig. 11). The structure with the carbonyl oxygen of that acetyl group 'left down', was found to be unstable, always returning to the 'left up' global minimum conformer.

The TDDFT-based overall UV spectrum of **3** (Fig. 12) reproduced the experimental UV curve with a reasonable accuracy, so that no UV correction was necessary. Comparison of the respective CD spectra predicted for the two enantiomers of **3** (for comparison of the single CD curves of the individual conformers, see Fig. S4) clearly showed that the more rapidly eluting peak, corresponding to the major product, has the *P*-configuration, as expected, and the minor, more slowly eluting enantiomer is *M*-configured.

For the computationally costly DFT/MRCI CD calculations, several simplifications had to be applied. Due to its almost negligible impact (2%, Fig. 11) in the overall CD spectrum, the third conformer (*conf 3*, O_{Ac} 'right down') was not considered; furthermore, for the remaining two minimum structures, all *O*-methyl groups in the anthracene part of the molecule and one of the OMe group at C-6′ in the acetylphloroglucinol ring were manually replaced by a hydrogen atom each (**3′**, Fig. 12), since only a molecule with fewer than 250 electrons could be treated by the MRCI/SVP calculations. Moreover, exemplarily for the global minimum conformer (*conf 1*), it was proven by B3LYP/TZVP calculations that such a replacement does not change the resulting CD spectrum (for the respective spectral comparison, see Fig. S5 in Supplementary data), and hence the overall CD spectra calculated for (*P*)- and (*M*)-**3′** can be safely compared with the experimental curves of the 'leuco' phenylanthracene derivative **3**. The excitation energies calculated by the DFT/MRCI/SVP method for **3′** were again

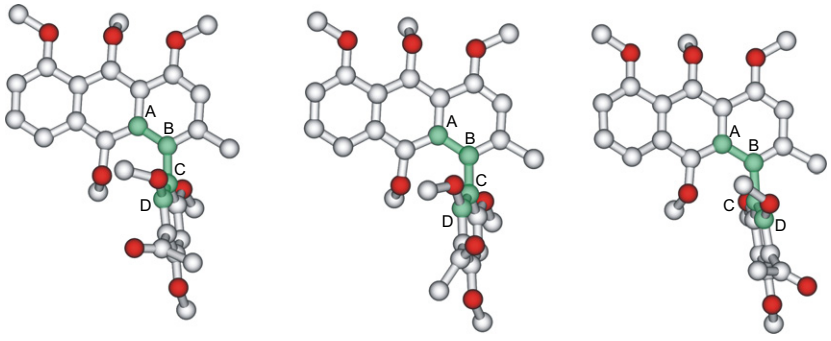

conf1 (θ_{ABCD} -93°) O_{Ac} 'left up'

conf2 (θ_{ABCD} -73°) O_{Ac} 'right up'

conf3 (θ_{ABCD} -101°) O_{Ac} 'right down'

$\Delta\Delta H_f$[kcal/mol]	*conf1*	*conf2*	*conf3*
BLYP/SVP	0.00	-0.09	2.15
BLYP/TZVP	0.00	0.68	1.55
B3LYP/TZVP	0.00	1.09	2.09
g_i^{B3LYP}	0.72	0.25	0.02

Figure 11. The energetically lowest-lying conformers of the 'leuco' derivative **3** of knipholone (**1**) with their relative energies and the weighting factors calculated from the B3LYP energies.

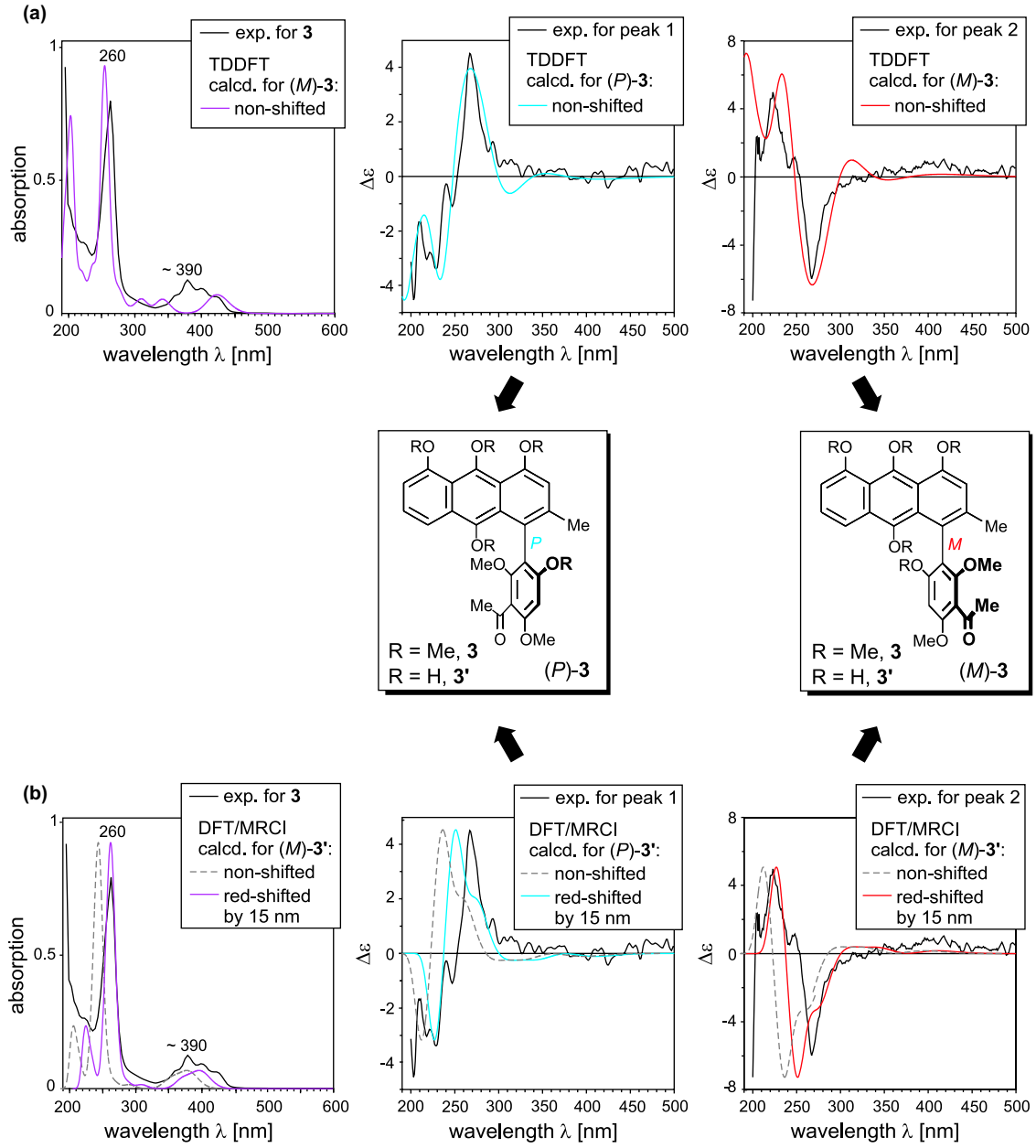

Figure 12. Assignment of the absolute axial configuration of the 'leuco' phenylanthracene derivative **3** by comparison of the online experimental CD spectra of the two peaks with the theoretically predicted CD curves, as deduced from the results of the TDDFT (a) and of the DFT/MRCI (b) calculations.

overestimated by 0.3 eV (about 15 nm) as compared to the experimental UV bands at 390 and 260 nm. This energy shift, which seems to be systematic for such large biaryl systems, might be probably diminished by increasing the configuration-selection threshold (δE_{sel}) from 0.8 to 1.0[36] or by using a larger basis set including diffuse functions.

Nevertheless, the DFT/MRCI/SVP based CD spectrum predicted for the *P*-enantiomer of **3′** showed a strong first positive Cotton effect followed by a second negative one, which was in a good agreement with the CD features of the first eluting peak of **3**, whereas the spectrum calculated for (*M*)-**3′** clearly reproduced the CD curve of the second peak.

The above investigations clearly prove that (*P*)-(+)-knipholone (**1**), according to the new configurational assignment, does result in the *P*-configured 'leuco' derivative **3**, and vice versa, (*M*)-(−)-**1** gives the *M*-atropo-enantiomer of **3**, thus fully supporting the new, revised configurational assignment for these phenylanthraquinone natural products.

3. Conclusion

The absolute axial configuration of the naturally occurring phenylanthraquinones, knipholone (**1**) and knipholone anthrone (**2**), was re-investigated by quantum chemical CD calculations showing that the previous assignment, based on merely semiempirical calculations (in combination with not entirely pure samples, due to instability reasons) had been erroneous. The renewed CD calculations using highly advanced methods, viz. TDDFT and DFT/MRCI,

unequivocally prove that the naturally predominant, dextrorotatory forms of knipholone, (+)-**1** (which is the more rapidly eluting enantiomer on a Chiralcel OD-H phase), and of knipholone anthrone, (+)-**2** (i.e., the more slowly eluting enantiomer on the same phase), have the *P*-configuration at the biaryl axis (Scheme 3). Consequently, the laevorotatory antipodes, (−)-**1** (i.e., the more slowly eluting peak) and (−)-**2** (the faster eluting one), which likewise exist in nature, are *M*-configured. Although with a certain degree of racemization, (+)-**1** can be converted into (+)-**2** and vice versa (Scheme 3), showing that the two compounds are stereochemically identical, which is in agreement with the quantum chemical CD calculations, according to which they both are *P*-configured. A third, again independent assignment results from the additional configurational attribution of the phenylanthracene (+)-**3**, which, without substantial loss of enantiomerical purity, can be obtained from (+)-**1** by O-methylation, reduction, and renewed O-methylation, again giving a *P*-configured product according to the CD calculations, so that all the three approaches jointly prove the *P*-configuration of **1** and **2** in the dextrorotatory series.

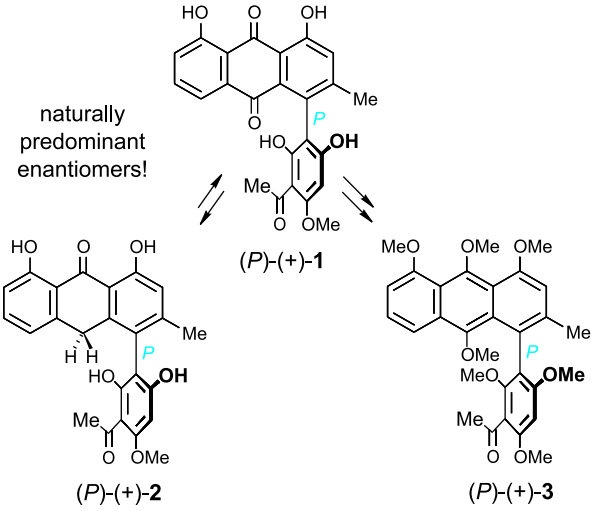

Scheme 3. Revised absolute stereostructures of the natural phenylanthraquinones, (+)-knipholone [(+)-**1**], and (+)-knipholone anthrone [(+)-**2**], and structure of the synthetically produced 'leuco' phenylanthracene derivative (+)-**3** and their stereochemical identity evidenced through interconversion.

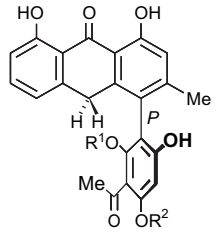

	R^1	R^2	axis
2[10,12]	H	Me	*P*
8[27]	Me	H	*P*

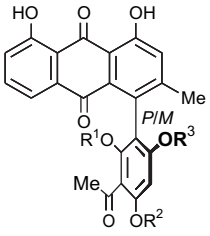

	R^1	R^2	R^3	axis
1[10,12]	H	Me	H	*P*
9[27]	Me	H	H	*P*
10[12]	H	Me	Me	*M*
11[67]	H	H	Me	*M*
12[12]	H	H	H	*P*

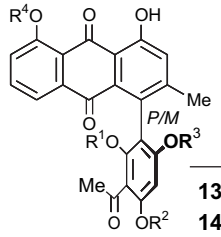

	R^1	R^2	R^3	R^4	axis
13[68]	Glc	H	H	H	*P*
14[49]	H	Glc	H	H	*P*
15[5]	H	Me	Glc	H	*M*
16[5]	H	H	Xyl	H	*M*
17[69]	H	Me	H	Glc-(1→6)-Glc	*P*

Glc = β-D-glucose
Xyl = β-D-xylose

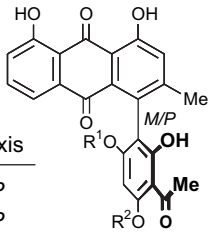

	R^1	R^2	axis
18[5]	H	Glc	*M*
19[5]	H	Xyl	*M*
20[5]	H	Glc-(1→3)-Xyl	*M*
21[9]	SO_3Na	Me	*P*

Glc = β-D-glucose
Xyl = β-D-xylose

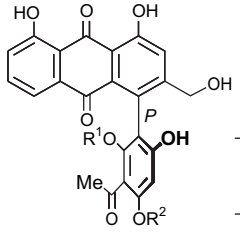

	R^1	R^2	axis
22[49]	Me	H	*P*
23[49]	H	Me	*P*

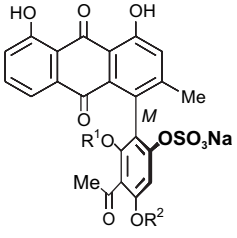

	R^1	R^2	axis
24[9]	Me	H	*M*
25[9]	H	H	*M*
26[9]	H	Glc	*M*

Glc = β-D-glucose

Figure 13. Absolute stereostructures of further phenylanthraquinones,[59] as deduced from their published CD data in correlation with the CD spectra of **1** and **2** as the parent compounds, and their revised assignment. Note that compounds **15** and **16**, although stereochemically analogous to (*P*)-**1**, possess the *M*-configuration due to the Cahn–Ingold–Prelog formalism and have been erroneously denoted in the literature;[5] therefore and because of the revision performed in this paper the descriptors of **15** and **16** have to remain the same.

The 'knipholone story' shows that even slight doubts about a structural assignment (here the attribution of the axial configurations of **1** and **2**) inevitably have to trigger further efforts to either verify or falsify an attribution initially made. In the present case, this revision was hampered, for years, by the unfavorable crystallization properties of knipholone (**1**) and its derivatives (which either did not crystallize or only in a racemic form) and by the lacking possibility of assigning axial configurations relative to chiral auxiliary centers, naturally present (like in naphthylisoquinoline alkaloids, e.g., dioncophylline A[57] or in dimeric pre-anthraquinones, like phlegmacins[58]) or artificially introduced, e.g., through NOESY measurements. For all these reasons, the only remaining possibility was the method of quantum chemically predicting the CD spectra, although this (at the level of 1998/1999) had been exactly the method that had initially failed. The previously erroneous assignment shows that for calculating such molecules with structurally challenging chromophores (here the anthraquinone and acetophenone portions), great caution is needed when using only semiempirical methods. Still, the work demonstrates that it is worth the effort to invest the required time and energy into such a revision, even if (hopefully) in the end the old assignment can 'only' be verified.

Since knipholone (**1**) and its anthrone **2** are the key representatives within the class of the naturally occurring phenylanthraquinones, the now reliable knowledge of their stereostructures is of highest importance for a further improvement of their bioactivities (e.g., concerning the atropisomer-dependent antitumoral activity[5]) and, based on the known CD data, for the now possible stereochemical re-assignment of virtually all other naturally occurring phenylanthraquinones. Their structures, as evident from the present work, are seen in Figure 13.

Through the revision of the absolute stereostructures of **1** and **2**, our 'lactone method' for the atropo-enantioselective synthesis of axially chiral biaryls, by the directed, enantiodivergent ring cleavage of chiral, but configurationally unstable bridged biaryl lactones by using the CBS system, has now indeed become a stereochemically fully consistent method. Thus, the previous assumed gap has been closed, and the method can now even be used for the configurational assignment of absolute axial configurations of as yet unknown biarylic compounds.

4. Computational

4.1. Conformational analysis

The detailed conformational analyses of the *M*-enantiomers of knipholone (**1**), knipholone anthrone (**2**), and the phenylanthracene **3** were carried out at the semiempirical PM3[37] level within the GAUSSIAN 03[60] program package, starting with geometries pre-optimized by the TRIPOS[61,62] force field. The obtained conformers were further optimized by DFT-based methods, viz. RI-BLYP/SVP[38,39,41] and B3LYP/TZVP,[40,43,44] within the TURBOMOLE 5.8[63] suite of programs.

4.2. CD calculations

The excited-state energy calculations were performed with the TDDFT (B3LYP/TZVP)[43,44] method and with the DFT/MRCI (BHLYP/SVP)[36] approach resulting in the excitation energies, oscillator, and rotatory strengths for the energetically lowest 80 and 35 excited states, respectively. To reduce the computational costs of the DFT/MRCI computations, a configuration-selection cut-off of $0.8E_h$ was used.[46] For acquiring the UV and CD spectra, the dipole–velocity representation[64] of the oscillator and rotatory strengths was chosen.

The line-shape CD curves $\Delta\varepsilon(\lambda)$ were obtained from the 'bar-type' spectra of **1–3** by utilizing a Gaussian distribution[65] according to

$$\Delta\varepsilon(\lambda) = \frac{1}{2.297\times10^{-39}}\frac{1}{\sigma\sqrt{2\pi}}\sum_i \lambda_k R_{0k}\exp\left[-\frac{(\lambda-\lambda_k)^2}{2\sigma^2}\right],$$

where λ_k and R_{0k} are the wavelength and the rotatory strength of the *k*th electronic transition, respectively, and σ is the exponential half-width, i.e., half the width of the CD band at $1/e$ height. For the CD spectra calculated by both TDDFT and DFT/MRCI methods, the empirically chosen σ values of 0.1 (for **2**), 0.15 (for **1**), and 0.2 eV (for **3**) were used. In the case of the UV spectra, a value of 0.1 eV was applied for all compounds. For compounds **1** and **3**, the single CD and UV spectra calculated for the individual conformers were added up according to their B3LYP/TZVP energies, following the Boltzmann statistic. The CD curves of the corresponding *P*-enantiomers of **1–3** were obtained by reflecting the spectra calculated for the *M*-configured isomers at their zero-line.

5. Experimental

5.1. General

All reagents used were reagent grade and solvents were distilled prior to usage. Analytical TLC was performed on Merck pre-coated silica gel 60 F_{254} plates. Compounds on TLC were visualized under long (365 nm) and short (254 nm) UV light. Column chromatography was performed using Merck silica gel (0.063–0.2 mm). Preparative HPLC was achieved on a Chromolith RP_{18} column (100× 10 mm). Stereoanalytical separations were carried out on a chiral stationary phase employing a Chiralcel OD-H HPLC column (4.6×250 mm, particle size: 5 μm) from Daicel Chemical Industries Ltd (Tokyo, Japan).

Melting points were determined on a Reichert-Jung Thermovar hot plate and are uncorrected. Optical rotations were measured on a JASCO P-1020 polarimeter. UV/vis spectra were obtained on a Cary 50 Conc spectrometer (Varian). The relative UV intensities at the given wavelength λ [nm] are reported referring to the most intense absorption band. IR spectra were measured on a Jasco FTIR-410 spectrometer. NMR spectra were recorded on a Bruker AV 400 (400 MHz) and a Bruker A 250 (250 MHz). All NMR

measurements were carried out at room temperature in deuterated acetone or methanol. Chemical shifts are reported as part per million (ppm) in δ units relative to the resonance of residual acetone (2.09 ppm in the ^{1}H, 29.82 ppm in the ^{13}C spectra) and methanol (3.34 ppm in the ^{1}H, 49.02 ppm in the ^{13}C spectra). Coupling constants (J) are reported in hertz [Hz]. Splitting patterns are described as 's' (singlet), 'd' (doublet), 't' (triplet), and 'm' (multiplet). ^{1}H NMR data are reported in the following order: chemical shifts, multiplicity, coupling constant, and number(s) of proton. CD spectra were recorded on a J-715 spectrometer (JASCO Deutschland, Gross-Umstadt, Germany) at room temperature using 0.05 and 0.1 cm standard cells and spectrophotometric grade MeOH, *n*-hexane, or a mixture of CH_3CN/H_2O (60:40) and are reported in $\Delta\varepsilon$ in units of cm^2/mol at the given wavelength λ [nm]. For HPLC–CD coupling experiments, the J-715 spectropolarimeter was equipped with a PU-1580 pump (JASCO), an LG-980-02S ternary gradient unit, a 7725i Rheodyne injector valve, an ERC-7215 UV detector hyphenated to a J-715 spectropolarimeter with a 0.5 cm standard flow cell, and the Borwin chromatographic software (JASCO Deutschland). ESI-HRMS were recorded on a microTOF-focus (Bruker Daltonik GmbH) (positive ionization, capillary temperature 210 °C, voltage 3.5 kV, and with nitrogen as the nebulizer gas).

5.1.1. Oxidative conversion of knipholone anthrone (2) to knipholone (1). According to a procedure described by Dagne and Yenesew,[2] synthetically produced[12] enantiomerically pure (+)-knipholone anthrone (2.4 mg, 5.71 μmol, 100:0 *P* to *M*, Fig. 9) in 5% methanolic KOH (5 mL) was stirred overnight in the presence of air. The resulting red mixture was acidified with 2 N HCl followed by dilution with water and extraction with EtOAc. After drying with $MgSO_4$ and evaporation of the solvent in vacuo the obtained residue was purified on a Chromolith RP_{18} column (100×10 mm) using H_2O (A)/CH_3CN (B); flow rate 10 mL/min; 0 min 5% B, 5 min 50% B, 9 min 100% B, 11 min 100% B, 11.5 min 100% B, 12 min 5% B, and 15 min 5% B, giving (+)-knipholone (2.36 mg, 5.44 μmol, 95%, 69:31 *P* to *M*) identical to an authentic sample (by co-TLC, co-HPLC, and ^{1}H NMR).

5.1.2. Conversion of knipholone (1) to knipholone anthrone (2). Following a method by Auterhoff and Scherff,[66] a mixture of knipholone (4.2 mg, 9.68 μmol, 75:25 *P* to *M*), glacial acetic acid (4 mL), and 40% $SnCl_2$ solution in concentrated HCl (4 mL) was heated at 120 °C for 2 h. After cooling, the resulting solution was poured into brine (20 mL) and exhaustively extracted with EtOAc, dried ($MgSO_4$), and the solvent was removed under reduced pressure. The residue was purified on a short silica gel column, eluted with an increasing gradient of CH_2Cl_2/MeOH (100:1 up to 100:4) affording knipholone anthrone (1.5 mg, 3.57 μmol, 37%, 52:48 *P* to *M*) chromatographically and spectroscopically identical to an authentic sample (by co-TLC, co-HPLC, and ^{1}H NMR).

5.1.3. Knipholone tetramethylether (7). To a solution of knipholone (**1**) (5.1 mg, 11.8 μmol, 89:11 *P* to *M*), in a mixture of acetone (10 mL) and water (0.1 mL), Cs_2CO_3 (150 mg, 0.46 mmol) and dimethylsulfate (116 mg, 0.92 mmol) were added. The mixture was stirred for 2 h at room temperature. After addition of 25% aqueous ammonia (2.5 mL), the acetone was removed under reduced pressure and the aqueous layer extracted with Et_2O (3×30 mL). The organic layers were combined, dried over $MgSO_4$, and the solvent was evaporated in vacuo. The residue was chromatographed on silica gel (EtOAc/petroleum ether 11:1) to afford knipholone tetramethylether (**7**) (5.5 mg, 11.2 μmol, 95%, 89:11 *P* to *M*) as a yellow oil that solidified upon standing: mp 223 °C (lit.[1] 225 °C). ^{1}H NMR [250 MHz, $CO(CD_3)_2$] δ 2.17 (s, 3H), 2.53 (s, 3H), 3.31 (s, 3H), 3.69 (s, 3H), 3.97 (s, 3H), 4.00 (s, 3H), 4.03 (s, 3H), 6.59 (s, 1H), 7.44 (m, 3H), 7.67 (t, J=7.93 Hz, 1H); ^{13}C NMR (63 MHz, $CO(CD_3)_2$) δ 21.35, 33.12, 56.66, 56.93, 56.97, 62.08, 93.17, 108.32, 116.49, 118.40, 118.84, 120.01, 124.42, 125.56, 126.33, 134.82, 137.91, 147.04, 156.06, 158.38, 159.02, 159.41, 159.50, 169.38, 186.60, 201.19.

5.1.4. Reductive O-methylation of 7 to phenylanthracene 3. Sodium dithionite (7.0 mg, 40.0 μmol) was added under a nitrogen atmosphere at 0 °C to a solution of knipholone tetramethylether (**7**) (4.2 mg, 8.6 μmol, 89:11 *P* to *M*) and tetra-*n*-butylammonium bromide (1.1 mg) in tetrahydrofuran (5.0 mL) and water (3.0 mL). The mixture was stirred at 0 °C for 2 h. After addition of 2.0 N aqueous NaOH (0.50 mL, 1.0 mmol), the solution was stirred for another 30 min and dimethylsulfate (15.1 mg, 0.12 mmol) was added. The reaction mixture was warmed up to room temperature, stirred for further 6 h, and extracted with Et_2O (3×30 mL). The combined organic layers were dried over Na_2SO_4 and the solvent was removed in vacuo. The crude product was purified on a short silica gel column eluted with CH_2Cl_2/MeOH (100:0.5) followed by preparative HPLC on a Chromolith RP_{18} column (100×10 mm) using H_2O (A)/CH_3CN (B); 0 min 6 mL/min, 10% B; 0.5 min 10 mL/min, 10% B; 5 min 10 mL/min, 50% B; 9 min 10 mL/min, 100% B; 13 min 10 mL/min, 100% B; 14 min, 10% B; 14.5 min 6 mL/min, 10% B; 15 min 10% B; giving pure 'leuco' phenylanthracene **3** (2.4 mg, 4.4 μmol, 53%, 85:15 *P* to *M*) as a yellowish oil. $[\alpha]_D$ +17.93 (*c* 0.18, MeOH), 85:15 *P* to *M*; ^{1}H NMR (400 MHz, MeOD) δ 2.17 (s, 3H), 2.52 (s, 3H), 3.16 (s, 3H), 3.36 (s, 3H), 3.82 (s, 3H), 3.90 (s, 3H), 3.99 (s, 3H), 4.05 (s, 3H), 4.08 (s, 3H), 6.65 (s, 1H), 6.85 (m, 2H), 7.34 (dd, J=8.74, 7.52 Hz, 1H), 7.65 (dd, J=8.74, 0.84 Hz, 1H); ^{13}C (100 MHz, MeOD) δ 21.57, 32.90, 56.28, 56.69, 56.71, 56.77, 61.46, 62.90, 64.13, 92.29, 105.29, 108.95, 116.36, 119.10, 119.70, 119.91, 120.04, 120.16, 126.99, 128.89, 129.96, 138.00, 149.89, 151.27, 157.12, 157.68. 158.37, 158.39, 160.52, 205.17; UV/vis (MeOH): λ_{max} 419 (0.11), 399 (0.14), 379 (0.16), 263 (1.00), 227 (0.52); CD (MeOH): $\Delta\varepsilon_{206}$ −5.6, $\Delta\varepsilon_{222}$ −6.7, $\Delta\varepsilon_{245}$ ε0.7, $\Delta\varepsilon_{268}$ +9.8; IR (neat): ν_{max} 2924, 2852, 1576, 1415, 1115, 418 cm^{-1}; HRMS (ESI$^+$) found: [(M+Na)$^+$], 543.1989. $C_{30}H_{22}NaO_8$ requires [(M+Na)$^+$], 543.1995.

Acknowledgements

This work was supported by the Fonds der Chemischen Industrie and by the DFG project Br 699/13-5 ('Natural Products from African Medicinal Plants'). J.M.-C. acknowledges the Alexander-von-Humboldt Foundation for her Georg-Forster research fellowship. We are also grateful to

Prof. S. Grimme, Univ. of Münster, Germany for providing us with the software required for the DFT/MRCI calculations and to Dr. A. Yenesew, Univ. of Nairobi, Kenya for authentic samples of phenylanthraquinones.

Supplementary data

Results of the B3LYP/TZVP CD calculations on the RI-BLYP/SVP optimized structures of **1**. HPLC–UV and HPLC–CD diagrams of the spiking experiment. The CD spectra calculated for **3** and **3′** by the B3LYP/TZVP method. Supplementary data associated with this article can be found in the online version, at doi:10.1016/j.tet.2007.07.001.

References and notes

1. Dagne, E.; Steglich, W. *Phytochemistry* **1984**, *23*, 1729–1731.
2. Dagne, E.; Yenesew, A. *Phytochemistry* **1993**, *34*, 1440–1441.
3. Bringmann, G.; Noll, T. F.; Gulder, T.; Dreyer, M.; Grüne, M.; Moskau, D. *J. Org. Chem.* **2007**, *72*, 3247–3252.
4. Bringmann, G.; Menche, D.; Bezabih, M.; Abegaz, B. M.; Kaminsky, R. *Planta Med.* **1999**, *65*, 757–758.
5. Kuroda, M.; Mimaki, Y.; Sakagami, H.; Sashida, Y. *J. Nat. Prod.* **2003**, *66*, 894–897.
6. Habtemariam, S. *Food Chem.* **2007**, *102*, 1042–1047.
7. Wube, A. A.; Bucar, F.; Asres, K.; Gibbons, S.; Adams, M.; Streit, B.; Bodensieck, A.; Bauer, R. *Phytomedicine* **2006**, *13*, 452–456.
8. Bringmann, G.; Günther, C.; Ochse, M.; Schupp, O.; Tasler, S. *Progress in the Chemistry of Organic Natural Products*; Herz, W., Falk, H., Kirby, G. W., Moore, R. E., Eds.; Springer: Vienna, 2001; Vol. 82, pp 1–249.
9. Mutanyatta, J.; Bezabih, M.; Abegaz, B. M.; Dreyer, M.; Brun, R.; Kocher, N.; Bringmann, G. *Tetrahedron* **2005**, *61*, 8475–8484.
10. Bringmann, G.; Kraus, J.; Menche, D.; Messer, K. *Tetrahedron* **1999**, *55*, 7563–7572.
11. Bringmann, G.; Menche, D. *Angew. Chem., Int. Ed.* **2001**, *40*, 1687–1690.
12. Bringmann, G.; Menche, D.; Kraus, J.; Mühlbacher, J.; Peters, K.; Peters, E.-M.; Brun, R.; Bezabih, M.; Abegaz, B. M. *J. Org. Chem.* **2002**, *67*, 5595–5610.
13. Bringmann, G.; Breuning, M.; Tasler, S. *Synthesis* **1999**, 525–558.
14. Bringmann, G.; Breuning, M.; Pfeifer, R.-M.; Schenk, W. A.; Kamikawa, K.; Uemura, M. *J. Organomet. Chem.* **2002**, *661*, 31–47.
15. Bringmann, G.; Pabst, T.; Henschel, P.; Kraus, J.; Peters, K.; Peters, E.-M.; Rycroft, D. S.; Connolly, J. D. *J. Am. Chem. Soc.* **2000**, *122*, 9127–9133.
16. Bringmann, G.; Menche, D.; Mühlbacher, J.; Reichert, M.; Saito, N.; Pfeiffer, S. S.; Lipshutz, B. H. *Org. Lett.* **2002**, *4*, 2833–2836.
17. Bringmann, G.; Saeb, W.; Rübenacker, M. *Tetrahedron* **1999**, *55*, 423–432.
18. Bringmann, G.; Ochse, M.; Götz, R. *J. Org. Chem.* **2000**, *65*, 2069–2077.
19. Bringmann, G.; Menche, D. *Acc. Chem. Res.* **2001**, *34*, 615–624.
20. Bringmann, G.; Tasler, S.; Pfeifer, R.-M.; Breuning, M. *J. Organomet. Chem.* **2002**, *661*, 49–65.
21. Abe, H.; Takeda, S.; Fujita, T.; Nishioka, K.; Takeuchi, Y.; Harayama, T. *Tetrahedron Lett.* **2004**, *45*, 2327–2329.
22. Fletcher, S. P.; Dumur, F.; Pollard, M. M.; Feringa, B. L. *Science* **2005**, *310*, 80–82.
23. Takeda, S.; Abe, H.; Takeuchi, Y.; Harayama, T. *Tetrahedron* **2006**, *63*, 396–408.
24. Bringmann, G.; Pfeifer, R.-M.; Schreiber, P.; Hartner, K.; Schraut, M.; Breuning, M. *Tetrahedron* **2004**, *60*, 4349–4360.
25. Ohmori, K.; Tamiya, M.; Kitamura, M.; Kato, H.; Oorui, M.; Suzuki, K. *Angew. Chem., Int. Ed.* **2005**, *44*, 3871–3874.
26. Bringmann, G.; Vitt, D. *J. Org. Chem.* **1995**, *60*, 7674–7681.
27. Yenesew, A.; Wanjohi, J. M.; Midiwo, J. O.; Heydenreich, M.; Peter, M. G.; Brun, R.; Müller, W. E. G.; Maksimenka, K.; Mutanyatta-Comar, J.; Bringmann, G. Unpublished results.
28. Doub, L.; Vandenbelt, J. M. *J. Am. Chem. Soc.* **1947**, *69*, 2714–2723.
29. Shimada, R.; Goodman, L. *J. Chem. Phys.* **1965**, *43*, 2027–2041.
30. Dehler, J.; Dörr, F. *Tetrahedron Lett.* **1965**, *6*, 2155–2160.
31. Harada, N.; Nakanishi, K. *Acc. Chem. Res.* **1972**, *5*, 257–263.
32. Casida, M. E. *Recent Advances in Density Functional Methods*; Chong, D. P., Ed.; World Scientific: Singapore, 1995; pp 155–192.
33. Gross, E. K. U.; Dobson, J. F.; Petersilka, M. *Top. Curr. Chem.* **1996**, *181*, 80–172.
34. Furche, F.; Ahlrichs, R.; Wachsmann, C.; Weber, E.; Sobanski, A.; Vögtle, F.; Grimme, S. *J. Am. Chem. Soc.* **2000**, *122*, 1717–1724.
35. Crawford, T. D. *Theor. Chem. Acc.* **2006**, *115*, 227–245.
36. Grimme, S.; Waletzke, M. *J. Chem. Phys.* **1999**, *111*, 5645–5655.
37. Stewart, J. J. P. *J. Comput. Chem.* **1989**, *10*, 221–264.
38. Vahtras, O.; Almloef, J.; Feyereisen, M. W. *Chem. Phys. Lett.* **1993**, *213*, 514–518.
39. Becke, A. D. *Phys. Rev. A* **1988**, *38*, 3098–3100.
40. Lee, C.; Yang, W.; Parr, R. G. *Phys. Rev. B* **1988**, *37*, 785–789.
41. Bauernschmitt, R.; Häser, M.; Treutler, O.; Ahlrichs, R. *Chem. Phys. Lett.* **1997**, *264*, 573–578.
42. Koch, W.; Holthausen, M. C. *A Chemist's Guide to Density Functional Theory*, 2nd ed.; Wiley-VCH-GmbH: Weinheim, 2001.
43. Becke, A. D. *J. Chem. Phys.* **1993**, *98*, 5648–5652.
44. Schäfer, A.; Huber, C.; Ahlrichs, R. *J. Chem. Phys.* **1994**, *100*, 5829–5835.
45. Becke, A. D. *J. Chem. Phys.* **1993**, *98*, 1372–1377.
46. Diedrich, C.; Grimme, S. *J. Phys. Chem. A* **2003**, *107*, 2524–2539.
47. Bringmann, G.; Busemann, S. *Natural Product Analysis: Chromatography, Spectroscopy, Biological Testing*; Schreier, P., Herderich, M., Humpf, H.-U., Schwab, W., Eds.; Vieweg: Wiesbaden, 1998; pp 195–211.
48. Bezabih, M.; Motlhagodi, S.; Abegaz, B. M. *Phytochemistry* **1997**, *46*, 1063–1067.
49. Abegaz, B. M.; Bezabih, M.; Msuta, T.; Brun, R.; Menche, D.; Mühlbacher, J.; Bringmann, G. *J. Nat. Prod.* **2002**, *65*, 1117–1121.
50. Hui, C. W.; Mak, T. C. W.; Wong, H. N. C. *Tetrahedron* **2004**, *60*, 3523–3531.
51. Lu, L.; Chen, Q.; Zhu, X.; Chen, C. *Synthesis* **2003**, 2464–2466.
52. Tius, M. A.; Gomez-Galeno, J.; Gu, X.-Q.; Zaidi, J. H. *J. Am. Chem. Soc.* **1991**, *113*, 5775–5783.

53. Quast, H.; Fuchsbauer, H.-L. *Chem. Ber.* **1986**, *119*, 1016–1038.
54. Kraus, G. A.; Man, T. O. *Synth. Commun.* **1986**, *16*, 1037–1042.
55. Krohn, K.; Miehe, F. *Liebigs Ann. Chem.* **1985**, 1329–1335.
56. Winters, R. T.; Sercel, A. D.; Showalter, H. D. H. *Synthesis* **1998**, 712–714.
57. Bringmann, G.; Rübenacker, M.; Jansen, J. R.; Scheutzow, D. *Tetrahedron Lett.* **1990**, *31*, 639–642.
58. Müller, M.; Lamottke, K.; Steglich, W.; Busemann, S.; Reichert, M.; Bringmann, G.; Spiteller, P. *Eur. J. Org. Chem.* **2004**, 4850–4855.
59. The names of the phenylanthraquinones shown in Figure 13 are: (+)-knipholone (**1**),[10,12] (+)-knipholone anthrone (**2**),[10,12] isoknipholone anthrone (**8**),[27] isoknipholone (**9**),[27] (−)-6′-*O*-methylknipholone (**10**),[12] (+)-bulbine-knipholone (**11**),[67] (+)-4′-*O*-demethylknipholone (**12**),[12] (+)-4′-*O*-demethylknipholone-2′-β-D-glucopyranoside (**13**),[68] (−)-4′-*O*-demethylknipholone-4′-*O*-β-D-glucopyranoside (**14**),[49] (+)-bulbineloneside A (**15**),[5] (+)-bulbineloneside B (**16**),[5] knipholone-2-*O*-β-D-gentiobioside (**17**),[69] (−)-bulbineloneside D (**18**),[5] (−)-bulbineloneside C (**19**),[5] (−)-bulbineloneside E (**20**),[5] (−)-sodium *ent*-knipholone 6′-*O*-sulfate (**21**),[9] (+)-gaboroquinone A (**22**),[49] (+)-gaboroquinone B (**23**),[49] (−)-sodium isoknipholone 6′-*O*-sulfate (**24**),[9] (+)-sodium 4′-*O*-demethylknipholone 6′-*O*-sulfate (**25**),[9] and (−)-sodium 4′-*O*-demethylknipholone-4′-β-D-glucopyranoside 6′-*O*-sulfate (**26**).[9]
60. Frisch, M. J.; Trucks, G. W.; Schlegel, H. B.; Scuseria, G. E.; Robb, M. A.; Cheeseman, J. R.; Montgomery, J. J. A.; Vreven, T.; Kudin, K. N.; Burant, J. C.; Millam, J. M.; Iyengar, S. S.; Tomasi, J.; Barone, V.; Mennucci, B.; Cossi, M.; Scalmani, G.; Rega, N.; Petersson, G. A.; Nakatsuji, H.; Hada, M.; Ehara, M.; Toyota, K.; Fukuda, R.; Hasegawa, J.; Ishida, M.; Nakajima, T.; Honda, Y.; Kitao, O.; Nakai, H.; Klene, M.; Li, X.; Knox, J. E.; Hratchian, H. P.; Cross, J. B.; Bakken, V.; Adamo, C.; Jaramillo, J.; Gomperts, R.; Stratmann, R. E.; Yazyev, O.; Austin, A. J.; Cammi, R.; Pomelli, C.; Ochterski, J. W.; Ayala, P. Y.; Morokuma, K.; Voth, G. A.; Salvador, P.; Dannenberg, J. J.; Zakrzewski, V. G.; Dapprich, S.; Daniels, A. D.; Strain, M. C.; Farkas, O.; Malick, D. K.; Rabuck, A. D.; Raghavachari, K.; Foresman, J. B.; Ortiz, J. V.; Cui, Q.; Baboul, A. G.; Clifford, S.; Cioslowski, J.; Stefanov, B. B.; Liu, G.; Liashenko, A.; Piskorz, P.; Komaromi, I.; Martin, R. L.; Fox, D. J.; Keith, T.; Al-Laham, M. A.; Peng, C. Y.; Nanayakkara, A.; Challacombe, M.; Gill, P. M. W.; Johnson, B.; Chen, W.; Wong, M. W.; Gonzalez, C.; Pople, J. A. *GAUSSIAN 03, Revision D.02*; Gaussian: Wallingford, CT, 2004.
61. Clark, M.; Cramer, R. D., III; Van Opdenbosch, N. *J. Comput. Chem.* **1989**, *10*, 982–1012.
62. SYBYL; Tripos Associates: 1699 St. Hanley Road, Suite 303, St. Louis, MO 63144, USA, 2006.
63. Ahlrichs, R.; Bär, M.; Baron, H.-P.; Bauernschmitt, R.; Böcker, S.; Crawford, N.; Deglmann, P.; Ehrig, M.; Eichkorn, K.; Elliott, S.; Furche, F.; Haase, F.; Häser, M.; Horn, H.; Hättig, C.; Huber, C.; Huniar, U.; Kattannek, M.; Köhn, A.; Kölmel, C.; Kollwitz, M.; May, K.; Nava, P.; Ochsenfeld, C.; Öhm, H.; Patzelt, H.; Rappoport, O.; Rubner, O.; Schäfer, A.; Schneider, U.; Sierka, M.; Treutler, O.; Unterreiner, B.; Arnim, M. v.; Weigend, F.; Weis, P.; Weiss, H. *TURBOMOLE 5.8 ed.*; Universität Karlsruhe: Karlsruhe, Germany, 2005.
64. Harris, R. A. *J. Chem. Phys.* **1969**, *50*, 3947–3951.
65. Schellman, J. A. *Chem. Rev.* **1975**, *75*, 323–331.
66. Auterhoff, H.; Scherff, F. C. *Arch. Pharm.* **1969**, *293*, 918–925.
67. Bringmann, G.; Menche, D.; Brun, R.; Msuta, T.; Abegaz, B. M. *Eur. J. Org. Chem.* **2002**, 1107–1111.
68. Qhotsokoane-Lusunzi, M. A.; Karuso, P. *Aust. J. Chem.* **2001**, *54*, 427–430.
69. Qhotsokoane-Lusunzi, M. A.; Karuso, P. *J. Nat. Prod.* **2001**, *64*, 1368–1372. Note that the structures **1** and **2** must be interchanged in this article!